ingegneria sismica
International Journal of Earthquake Engineering
Anno XLIII - Num. 2 - 2026

Accurate Training Path of AI Assistant Teaching System for Frisbee Physical Education Classes in Private Colleges and Universities

Ziyang Guo[1], *Xiao Wang*[2,*] *and Aoxuan Xu*[3]

1 Sports Department, Shaanxi Fashion Engineering University, Xianyang, Shaanxi, 712046, China

2 School of Education, Shaanxi Fashion Engineering University, Xianyang, Shaanxi, 712046, China

3 School of General Education, Guangxi Vocational University of Agriculture, Nanning, Guangxi, 530000, China

SUMMARY: *In order to improve the teaching effectiveness and training personalization level of frisbee sports classes in private universities, this study proposes the use of automated detection technology for automatic measurement of frisbee sports training process. Firstly, the overall structure of the system covering the functions of physiological information detection and movement data detection was designed, and then the construction of the dataset of the AI teaching assistant application system for physical education classes was completed, from which the human skeletal key point data were extracted. Then the spatial and temporal relationships between joints were modeled using spatio-temporal graph convolutional networks. Finally, the skeletal coordinates are converted into joint angles, and the DTW distance is used as a parameter to define the action evaluation formula to evaluate the Frisbee sports action. Experiments show that the disc sports movement recognition accuracy of the AI teaching assistant system for disc sports classes in private colleges is more than 90%, and the error between the algorithmic score and the expert score is only 0.7 points, which can effectively correlate the relationship between the disc sports movement and the movement extension angle, which verifies the feasibility of the teaching assistant system in the auxiliary teaching of disc sports classes in private colleges and universities, and it can realize the accurate and personalized training of the students.*

KEYWORDS: *spatio-temporal graph convolutional network; action recognition; skeletal key point detection; dynamic time regularization; frisbee sports action evaluation*

1 Introduction

In recent years, in the physical education teaching activities in colleges and universities, in order to solve the problems of single content of physical education courses and single teaching means, and also to enhance the physical health of students, promote the healthy growth and overall development of students, and improve the interest of students in sports, colleges and universities continue to innovate, and actively introduce new sports to improve the participation of students in sports [1]. As an emerging sport, Ultimate Frisbee has been developing rapidly in the past decade, with an increasing number of enthusiasts, and many colleges and universities have set up Ultimate Frisbee clubs, opened Frisbee clubs, and offered Ultimate Frisbee courses [2].

*eduwangx@163.com
https://doi.org/10.65102/is2026843
Published: 30 April, 2026

According to incomplete statistics, there are more than 100 collegiate frisbee teams in China, including Tsinghua University, Peking University and other famous schools, and every year there are new colleges and universities to join the team, Tianjin Institute of Physical Education set up the first Ultimate Frisbee team Tianjin Speed team in 2005, which is the prelude for the development of Ultimate Frisbee sports in Tianjin colleges and universities [3]. 2013 the first Guangzhou college students Ultimate Frisbee competition. In 2013, the first Guangzhou University Ultimate Frisbee Tournament was held at Guangdong University of Foreign Studies (GDFS), and the following year, the 1st Guangzhou University Mixed Group Tournament was held at GDFS. Although the development of Ultimate Frisbee has shown a booming trend, there are still many private colleges and universities in the region that have not come into contact with or even heard of this sport, and compared to Europe and the United States, as well as Hong Kong and Taiwan, the development and popularization of Ultimate Frisbee in China's private colleges and universities still has a long way to go [4].

With the rapid advancement of global technology, the field of education should also update and integrate advanced technologies, and it is also introducing various forms of intelligent assisted teaching systems to improve students' learning effectiveness and interest [5]. For example, Wang et al. modeled knowledge points and courses by combining the results of learners' learning and answering questions, based on which they proposed a strategy for presenting knowledge graphs and guiding learners through topological maps to provide personalized learning paths for learners [6]. According to Olędzka et al, AI technologies are rapidly integrating into the modern education system as an indispensable and critical tool, whose main roles include supporting personalized learning paths, optimizing teaching strategies, and enhancing students' critical thinking skills [7]. Almusawi et al. investigated teachers' attitudes towards the use of wearable devices in the physical education classroom, demonstrating that these technologies hold educational promise in the areas of teacher-student interaction, engagement, assessment, and feedback, and offer innovative and practical solutions for physical education [8]. Paiva and Bittencourt use a virtual teaching assistant system to find scenarios from a large amount of data that are similar to the teacher's current situation, and their predefined solutions for different teaching scenarios are designed to help teachers understand the situation and solve problems [9]. Chen et al. proposed an artificial intelligence based assistive teaching system that combines a question and answer (QA) system, an extension mechanism, a caching mechanism, and an error correction mechanism to assist the students' learning process and the instructor's teaching process [10]. Chandrakant in his study pointed out that AI technology significantly improves the teaching efficiency of educators, especially in managing teaching tasks showing higher effectiveness, emphasizing that traditional methods are no longer able to meet the needs of modern education, prompting the necessity of developing the development of AI teaching assistant systems based on Natural Language Processing (NLP) technology [11]. Zhang et al. designed an AI teaching assistant system called “i-assistant”, which contains four modules: cognitive level, subject competence, classroom status, and subject design and assessment, and combines intelligent algorithms with the classroom in order to assist teachers to teach accurately [12]. Yang et al. proposed an Artificial Intelligence-based Intelligent Teaching Assistant (ITA) system, and found that the ITA system's personalized learning paths, question-and-answer functions, and affective support measures not only enhanced students' motivation and engagement, but also effectively compensated for the deficiencies of the traditional online courses and improved students' learning outcomes [13].

In the field of physical education teaching, ZhaoriGetu and Li introduced a training method based on an improved convolutional neural network (RCNN) and biomechanical feedback in physical training. This method uses high-speed cameras and motion capture systems to capture biomechanical responses, enabling learners to correct incorrect postures on their own without

the need to hire professional coaches. Enhance students' enthusiasm for training [14]. Gao proposed a smart public physical education teaching method based on artificial intelligence technology, which assists in the development of a scientific exercise program through accurate exercise data analysis, enabling personalized teaching and thus promoting healthy physical and mental development [15]. Huang and Li proposed a personalized training method for taekwondo based on deep learning by establishing a data model matching each student's learning performance in order to achieve the personalized learning effect, and practice has shown that this personalized training program significantly improves the athlete's technical level and competition performance [16]. Liu et al. proposed an intelligent and precise teaching model applied to physical education teaching, which includes haptic interactive games, intelligent virtual teachers, catechism classes, and teaching aids such as heart rate monitoring, and the practice showed that the model was significantly improved in terms of learning interest, exercise duration, physical fitness, and independent learning ability compared with the traditional teaching model [17]. Xie proposed an innovative approach to physical education teaching based on intelligent vision technology, which is innovative in terms of teaching content, methods and means, aiming to enhance physical fitness and promote the physical and mental health development of young people, as well as to continuously cultivate students' interest in learning, thus motivating them to participate in physical exercise [18]. In Ultimate Frisbee training, Yeo and Chew proposed a computer vision and deep learning human activity recognition model based on computer vision and deep learning for throwing action training for beginners in Ultimate Frisbee, which lays the foundation for an automated coaching system that provides immediate feedback and accelerates the learning process for beginners [19].

Existing sports AI teaching assistant systems are mostly aimed at a single technical link, this study uses intelligent technology to obtain students' physiological information, sports equipment data, respectively, and on the basis of multi-dimensional data acquisition, obtains the key sequences of human joint points from the captured video of Frisbee sports class, and uses the excellent fitting ability of spatio-temporal graphic convolutional network to model the temporal-spatial graph between human joints. The cumulative distance of each joint angle curve and template of the dynamic time regularization algorithm is utilized. Realize the objective evaluation of frisbee action standardization. The scientificity of the action recognition algorithm and the evaluation algorithm are verified respectively through comparative experiments, and then relevant experiments are designed using intelligent tools such as Frisbee launchers to verify the feasibility of the AI teaching assistant system to realize accurate training paths in Frisbee physical education classes of private colleges and universities.

2 AI Assistant Teaching System for Frisbee Physical Education Classes in Private Colleges and Universities

2.1 Overall design

In order to be able to analyze the error objectively, the AI assistant teaching system for frisbee sports classes in private universities is designed based on big data. The main components of the system include the controller, physiological information detection system, sports equipment data detection system, movement data detection system, database and so on. The structure sketch of this private college frisbee sports class AI teaching assistant system is shown in Figure 1.

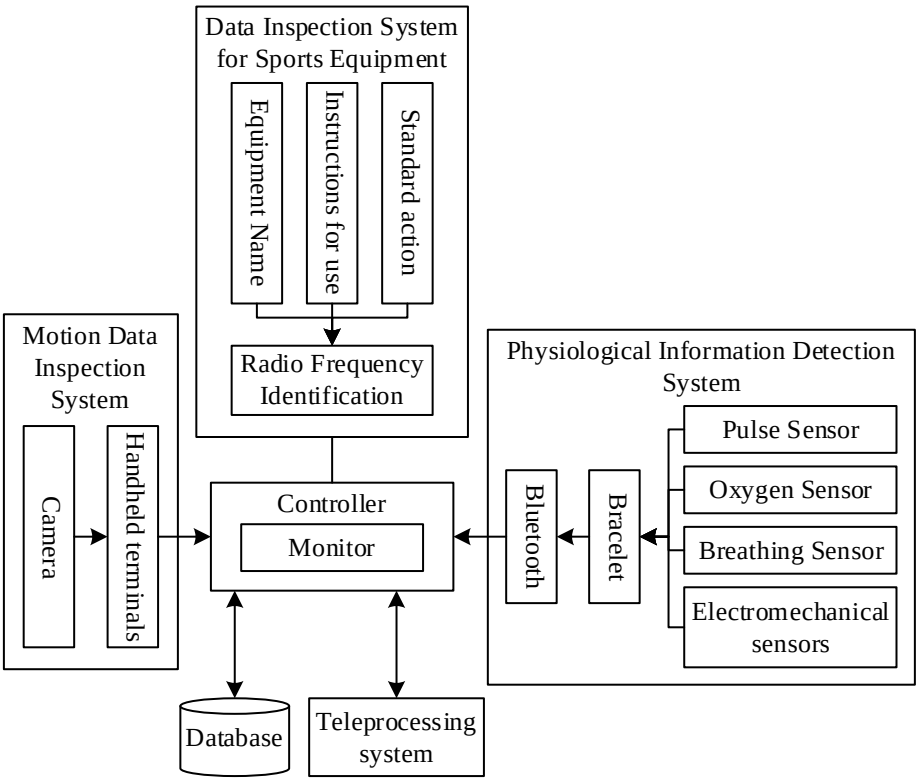

Figure 1: Flight disc sports training error detection system structure

2.2 Physiological information detection system

Physiological information detection system is mainly used to monitor the user's physical state, the data will be transmitted to the network of big data, according to the current user's physical state of the presumption of sports training can be achieved and the presumption of the future degree of training, for the system to carry out error analysis to make preparations. Physiological information detection system mainly through the installation of pulse, blood oxygen, respiration, electromyography sensors on the user's bracelet, real-time collection of the user's physical state, in order to make timely reminders in the training process, in order to prevent the emergence of accidental conditions, these physiological information through the Bluetooth transmission to the handheld terminal.

The pulse is determined by measuring the PPG signal of the human body, which is detected by optical means, i.e., two photoelectric probes are installed on the bracelet, one of which is a light probe that can emit green light at a constant rate, and the light emitted by the human body is reflected and then acts on the second light-sensitive probe, which converts the light signal into an electrical signal, i.e., the PPG signal, and the DC portion of the PPG signal is a stable signal, and the AC portion of the PPG signal is the pulse of the human body that is measured. The DC portion of the PPG signal is the stabilized signal, and the AC portion is the measured pulse rate of the body.

Blood oxygen is one of the indicators of the metabolic state of the human body, high blood oxygen means good metabolism, low blood samples means higher risk of cardiovascular diseases. Blood oxygen is monitored by an oxygen sensor chip and photodiode installed inside the bracelet. The chip emits red light and infrared light, when passing through the human blood, oxygen mainly absorbs red light, hemoglobin mainly absorbs infrared light, by calculating the difference in light intensity between the emitted and received by the photodiode can be

determined by the human body's blood oxygen content.

Breathing is one of the most important indicators of whether a person is healthy or not, and its rate and depth can effectively reflect a person's mood, movement and physiological state. There are many kinds of detection methods, such as thermal method, gas flow method, etc. However, in order to facilitate the movement, this system adopts the impedance method for measurement. During exercise, only need to put the two poles patch on both sides of the chest cavity, using the potential difference between the two poles can get the respiratory rate.

In the respiration rate and depth measurement, the alternating current is applied to the human body through the protective resistor R_P, and enters the chest cavity through the resistor and capacitor connected in parallel, and the final voltage measurement changes due to the change of resistance caused by the respiration in the chest cavity, and the respiration rate and depth can be determined by the change of value.

EMG signals reflect the movement of muscles, bones and nerves within the human body. By installing a myoelectric sensor inside the bracelet, the internal chip can monitor the analog electrical signals within the muscular system during human movement, thus monitoring the force generated by the process of muscle relaxation to contraction and back to relaxation.

2.3 Motion Equipment Data Detection System

In order to enable the error detection system to quickly identify the training errors when training in frisbee sports, it is first necessary to identify the method of training in frisbee sports. If you do not use the training equipment, it is directly on the action detection can be; if you use the relevant training equipment, the system needs to be able to quickly identify the name of the training equipment, the system uses radio frequency identification (RFID), through the user's bracelet on the read-write can quickly identify the name of the training equipment, the use of instructions, as well as other relevant commodity information, will read the equipment information and the user's log-in information, can quickly analyze the user's current training status, while the big data on the body's current training status, can be quickly analyzed, while the big data on the body's physical condition.

The internal device of radio frequency identification (RFID) mainly includes transponder, reader and support software.

When working, the transponder is mainly powered by DC power supply, firstly, the oscillator generates a stable frequency signal, which is sent to the modulator through the encoder, and then processed by the carrier generator to be expressed in the form of serial code, and finally the signal is coupled to the coil. The reader, on the other hand, first amplifies the weak signal after coupling, screens the signal for use through a demodulator, and the signal passes through a decoder and then uses a display circuit to show the received data.

2.4 Database

The database is used to store and manage all the data acquired by the system. The system database adopts MySQL database in tabular form, and this kind of database manages the data by using entity linkage diagram, which facilitates operations such as deletion or addition of data in the database. For this error detection system, its entity elements mainly include administrators, users, sports equipment, physiological information and action data, etc., and the attributes related to each entity element are associated with the entity elements to set up and manage the database. The entity linkage of this database is shown in Fig. 2.

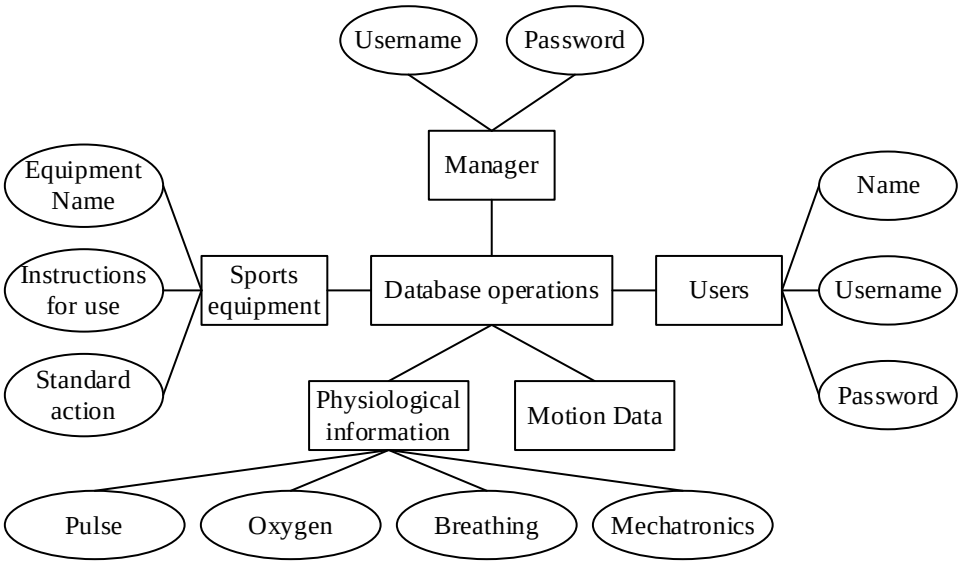

Figure 2: Entity connection of the database

3 Action recognition and evaluation algorithm based on human key point data

3.1 Frisbee Motion Recognition Dataset Construction

3.1.1 Raw Motion Data Acquisition

The construction of the frisbee motion action recognition dataset first requires raw motion video data acquisition. In this chapter, the video camera equipment is used to complete the video acquisition work and record all the frisbee sports actions involved in the program. Taking the frisbee sports program as an example, there are 9 types of actions in the frisbee sports program, which are basic throwing, advanced throwing, creative throwing, two-handed catching, one-handed catching, forehand catching, backhand catching, defense, and auxiliary technology. The video captured by the camera was segmented and processed to create separate video clips for each category of action, with a single action video duration of approximately 2 seconds and a video frame rate of about 60. The dataset consists of 100 video clips for each class of action, and each video file is named with the rule of “action class_video number”, and the videos of each class of action are put into the same action class folder, which is divided into the training set and the test set with the ratio of 8:2.

We crop all the video files into RGB image frames by OpenCV, and set all the image sizes to 320×240. At the same time, we obtain the segmentation information of all the image frames, add the category annotation information, and generate the annotated files for the training and testing sets, which is convenient for subsequent training and testing experiments on the video dataset.

3.1.2 Data set construction

The main research content of this section is the construction of skeletal dataset for frisbee sports action recognition, first of all, the target detection algorithm is used to locate the human body in the video, and the skeletal point coordinate information is extracted through the human body

posture estimation algorithm, and after the relevant data preprocessing operations, the final output is a serialized file for the experimental needs.

The specific implementation process of constructing the skeleton dataset is taken as an example of the Frisbee sports sports. First of all, the basic information of all video files (video name, action category, start frame number, end frame number) is obtained through Python, and the information is written into a JSON file, which is divided into a test set file and a training set file. The video list information is generated and computer vision tool libraries such as MMCV, MMDetection and MMPose are used to process the videos.

MMCV is a unified open base library introduced by OpenMMLab specifically built for different directions of computer vision, which supports a variety of algorithmic open source projects as well as a series of toolboxes, such as MMDetection for target detection, MMPose for pose estimation, and MMAction2 for action recognition, etc. MMCV provides a unified and extensible IO interface with image annotation and its visualization, image processing, video processing, multiple convolutional neural network models, and high-quality implementations of CPU and CUDA arithmetic.

MMDetection is a PyTorch-based target detection tool library in the OpenMMLab series, which supports the more mainstream target detection frameworks, and the basic detection frames and masks are implemented in the GPU version, and the training speed is faster or comparable to that of other codebases such as detectron2. In addition, MMDetection decouples the detection framework into different modular components, and users can customize the detection model according to their research needs.

MMPose is one of the open source frameworks of OpenMMLab project, which is an open source toolkit based on pose analysis, supporting mainstream pose analysis tasks in current academic research, including 3D human mesh recovery, 2D multi-person pose estimation, 2D face keypoint detection, etc. It supports the preparation and construction of mainstream datasets such as COCO, AIC, MPII, etc., and the model library supports most of the mainstream human posture algorithms, such as DeepPose, CPM, Hourglass, HRNet and so on.

The decord is used to decode the video information, call the improved FasterRCNN target detection model to locate the human position border in the picture, and then the HRNet human posture estimation model is used for the detection reasoning, and the human posture appearing in the video is detected in a top-down way, and the detected human skeletal point data are outputted, and according to the frisbee motion action category words in the name of the segmentation file to Label a set of skeletal point motion data, and merge the category labeling and skeletal data to produce a pickle format data file, forming a skeletal data set for frisbee motion action recognition in digital sports.

3.2 Action Recognition Algorithm Based on Learning Human Keypoint Data

3.2.1 Graph Convolutional Network Algorithm

Graph Convolutional Networks (GCN) are able to generalize Convolutional Neural Networks (CNNs) to non-Euclidean structures, which of course include skeleton maps. It has received widespread attention for its excellent performance on keypoint-based action recognition tasks.

The human keypoint data extracted from various actions in a frisbee player's competition, they contain a set of keypoint position coordinates and confidence levels for each frame of the image. For each frame, there are 17 human keypoints, corresponding to nose, left and right eyes, left and right ears, left and right shoulders, left and right elbows, left and right wrists, left and right hips, left and right knees, and left and right ankles, respectively. These points are naturally connected to form a human skeleton map, which is visualized as a human skeleton map.

Based on this information an undirected graph G is formed with the formula as:

$$G = (V, E) \tag{1}$$

where V denotes the set of nodes and E is the set of edges, in action recognition, it characterizes the human body keypoint information by considering the human body keypoints as nodes and the natural connections of the keypoints in the human body as edges. The convolution is computed based on the edges and the nodes they are connected to, and this method is more suitable for modeling human keypoint information than using sequence vectors or 2D images, as follows.

For a set of graph data, assume that there are N nodes, each node has its own D-dimensional feature vector, which can form an N × D-dimensional feature matrix X. In addition, each node will also form an N × N-dimensional adjacency matrix A between the nodes, which is used to represent the connectivity of each node, i.e., the human body's natural connectivity, X and A are the inputs of the graph convolutional network model.

For a node $H^{(l)}$ represents the feature vector matrix at layer 1 and $H^{(l+1)}$ represents the feature vector matrix after one convolution, and the formula for one convolution operation is as follows:

$$H^{(l+1)} = \sigma\left(\tilde{D}^{-\frac{1}{2}}\tilde{A}\tilde{D}^{-\frac{1}{2}}H^{(l)}W^{(l)}\right) \tag{2}$$

In this formula $\tilde{A} = A + I, I$ is the unit matrix, $\tilde{D}$ is the degree matrix of $\tilde{A}$, i.e., $\tilde{D} = \sum \tilde{A}_{ij}$, and H is the matrix of eigenvectors of all nodes of each layer, for the input layer $H^{(0)}$ is X, σ denoting the nonlinear activation function.

Graph Convolutional Networks utilize the matrix form to iteratively compute the features of each node, and the convolution operation is performed through layer propagation to obtain the final node features. However, graph convolutional network relies on the realization of multi-layer fully connected network, which is prone to overfitting phenomenon, and once it has too many layers, it is difficult to train out, usually the number of network layers should be within 6 layers. In addition, for the action recognition of frisbee scene, each action of the player during the game has a large amount of information in the time dimension, graph convolutional network only focuses on the spatial level of information, does not take into account the temporal level of inter-frame relationships, and can not deal with the spatio-temporal data very well. Spatio-temporal graph convolutional networks, on the other hand, can improve the prediction efficiency and accuracy of action recognition by constructing a local spatio-temporal graph and using the spatio-temporal graph convolution module to capture spatio-temporal correlation and heterogeneity.

3.2.2 Convolutional network algorithm for spatio-temporal maps

In order for action recognition to take into account information in the time dimension, we use a sequence of keypoints consisting of all the joints in each frame of the same frisbee player and use a spatio-temporal graph convolutional network to construct a spatio-temporal graph with the keypoints as the graph nodes, and the connectivity of the human body structure and time as the graph edges.

In the spatio-temporal graph convolutional network (STGCN), the hierarchical representation of the key point sequence is accomplished by the time-space graph.

Each layer of the spatio-temporal graph convolutional network, i.e., spatio-temporal graph convolutional module, consists of a spatial graph convolutional module (GCN) and a temporal graph convolutional module (TCN), of which the spatial graph convolutional module is the core part. A spatial graph convolution module followed by a temporal graph convolution module and residual structure is a layer of network. There are 10 layers in a spatio-temporal graph convolutional network, but the first layer does not have a residual structure, so it is often regarded as a 9-layer network, which can fit features better than graph convolutional networks, which usually have no more than 6 layers.

As input to the spatio-temporal graph convolutional network, the set of nodes $V=\{v_{ti} \mid t=1,2,\ldots,T, i=1,2,\ldots,N\}$, which, for the feature v_{ti} on the node, consists of the coordinates of the ith keypoint on the frame t, as well as the estimated confidence level, which is derived from the previous chapter, Body information in the sequence of keypoints.

As for the set of edges E, it consists of two subsets. The first one is the subset of spatial edges $E_S=\{v_{ti}v_{tj} \mid (i,j)\in H\}$, which represents the relationship between the keypoints in the same frame, where H is the set of naturally connected human joints. The second one is a subset of temporal edges $E_F=\{v_{ti}v_{(t+1)i}\}$, which denotes the relationship between keypoints of the human body between different frames, and thus all the edges in E_F of a particular joint i will denote its trajectory over time.

Up to this point, a graph containing spatial and temporal information is constructed based on a sequence of key points of a frisbee player's movements in a video. Among them, the node information is the horizontal and vertical coordinates and the confidence level; the edge information is E_s and E_F.

Before going deeper into the spatio-temporal graph convolutional formulation, the traditional convolutional network formulation is introduced here. For a given $\mathrm{K}\times\mathrm{K}$ convolution kernel and an input feature map f_{in} with a number of channels C, the formula for the output value of a single channel at position x, $f_{out}(x)$, is as follows:

$$f_{out}(x)=\sum_{h=1}^{K}\sum_{w=1}^{K} f_{in}(p(x,h,w))\cdot W(h,w) \tag{3}$$

The above formulation is then extended to the spatio-temporal graph, where node v is equivalent to x pixel points, in addition to defining the sampling function and the weighting function.

The sampling function is responsible for specifying the range of neighboring nodes involved in the graph convolution operation for each node, which is represented by the formula as in (4), where d denotes the distance between two nodes.

$$B(v_{ti})=\{v_{tj} \mid d(v_{tj},v_{ti})\le D\} \tag{4}$$

When $D=1$, i.e., it is to take only the first-order neighboring nodes, the sampling function samples only the directly neighboring nodes, and the formula is as in (5).

$$p(v_{it},v_{it})=v_{ij} \tag{5}$$

For the expansion of the weight function, it is first necessary to subset the neighboring nodes of a node in the graph, so that each subset has a label, and the neighboring nodes are mapped

to the subset labels it belongs to through l_{ti}. The weight function W represents the weight vector based on a node and its neighbors. Where $l_{ti}\left(v_{tj}\right)$ denotes the label to which v_{tj} belongs in the label of the subset of molecules with v_{ti} as the center node.

$$W\left(v_{ti},v_{tj}\right)=W'\left(l_{ti}\left(v_{tj}\right)\right) \tag{6}$$

In summary, the traditional convolution formula is expanded as:

$$f_{out}\left(v_{ti}\right)=\sum_{v_{tj}\in B(v_{ti})}\frac{1}{Z_{ti}\left(v_{tj}\right)}f_{in}\left(v_{tj}\right)\cdot W\left(l_{ti}\left(v_{tj}\right)\right) \tag{7}$$

Among them:

$$Z_{ti}\left(v_{tj}\right)=\left|\left\{\left(v_{tk}\mid l_{ti}\left(v_{tk}\right)=l_{ti}\left(v_{tj}\right)\right\}\right| \tag{8}$$

is the normalization term, i.e., the base of the corresponding subset, which is used to balance the contribution of different subsets.

Finally, to further expand on the time dimension, the concept of neighboring nodes of a node in the graph is mentioned earlier, and its definition formula on the spatio-temporal graph convolution is:

$$B\left(v_{ti}\right)=\left\{v_{qj}\mid d\left(v_{ti},v_{ti}\right)\le K,\mid q-t\mid\le[\Gamma/2]\right\} \tag{9}$$

From the above equation, it can be seen that the definition of neighboring nodes becomes less than K in spatial distance, and successively less than $[\Gamma/2]$ in inter-frame distance, i.e., temporal constraints are added to the definition of spatial neighborhood.

And the sampling function and weight function are the same as before on the added time-space graph convolutional network, only need to replace l_{ST} with the new label l_{ti}, the formula is as follows:

$$l_{ST}\left(v_{qj}\right)=l_{ti}\left(v_{tj}\right)+(q-t+[\Gamma/2])\times K \tag{10}$$

Compared with the graph convolutional network that only performs spatial convolution, the spatio-temporal graph convolutional network constructs a subset of temporal edges, which can better utilize the spatio-temporal information in the sequence of keypoints, and thus improves the accuracy and robustness of action recognition, which is more in line with the needs of this paper.

3.2.3 Performance Comparison of Recognition Schemes

In the case of uneven distribution of data volume, there is a huge drawback in using only the accuracy rate as an algorithm evaluation metric. In order to compare the two action recognition models based on features and based on deep learning more reasonably, the prediction error metrics used are introduced as follows:

(1) Confusion matrix

Taking the simplest binary classification problem in the classification model as an example,

the class of interest is usually labeled as positive class, and the other classes are negative classes, and the predicted output of the model is a binary judgment, i.e., “positive” or “negative”.

For the collection of test samples, we can directly know which data in the real situation of the actual label for the positive, which data for the negative, and then the sample data using the trained classification model for prediction, you can get the model that these data which is positive, which is negative.

Record the number of times each of these situations occurs, and so you get four basic numerical indicators, also known as the first level indicators (the lowest level):

TP - the number of times the positive class is predicted to be a positive class

FN - number of times the positive class is predicted to be a negative class

FP - the number of times the negative class is predicted to be a positive class

TN - the number of times a negative category is predicted to be a negative category

Summarizing these four first-level metrics together in tabular form gives the confusion matrix.

When evaluating a classification model, it is obvious that the model is expected to have a high rate of correct recognition, which corresponds to the confusion matrix, i.e., it is expected to have a large number of TPs and TNs and a small number of FPs and FNs. So after obtaining the confusion matrix of the model one should observe the distribution of the values in the four quadrants, the larger the values corresponding to the positions in the second and fourth quadrants, the better, and conversely, the smaller the values corresponding to the positions in the first, third and fourth quadrants, the better.

As for the multi-classification problem under this topic, the establishment of confusion matrix needs some extension. For the N-element categorization problem, the scale of the confusion matrix is $\mathrm{N}\times\mathrm{N}$, where each column represents the predicted category and each row represents the actual category.

Similar to the binary classification problem, we want the multivariate confusion matrix to be as large as possible on the diagonal and as small as possible in other positions.

(2) Accuracy

Accuracy rate refers to the proportion of correctly categorized samples to all samples, which is calculated from the first level index, so it is called the second level index, and the definition of accuracy rate is as follows:

$$P = \frac{TP}{TP + FP} \tag{11}$$

For the multivariate classification problem, the accuracy rate indicator can be calculated separately for each category by relabeling the current category of interest as positive and the other categories as negative. Therefore, the obtained metrics are N-element arrays.

The precision rate is usually used to evaluate the quality of the classification model.

(3) Recall rate

Recall rate, as the name suggests, refers to the proportion of target categories recalled among the categories of interest. Recall rate is a metric corresponding to precision rate, which is often used to evaluate the completeness of recognition results. The definition of recall rate is shown below:

$$R = \frac{TP}{TP + FN} \tag{12}$$

(4) The F_1 metrics

We want the recognition models to have the highest possible values for both precision and recall, but there is a contradiction between these two metrics.

Models with high recall have low precision, while models with high precision tend to have low recall. In order to weigh the impact of the two metrics, the two metrics are fused into a single metric, and a three-level metric, the F_1 metric, is obtained. The definition is shown in equation (13):

$$F_1 = \frac{2TP}{2TP + FP + FN} \tag{13}$$

The following action prediction experiments are performed by applying a combination of two window segmentation algorithms and two recognition models on the frisbee action dataset, respectively. The performance metrics of each type of action are weighted and averaged with the number of actions as weights, and the precision, recall and F1 metric scores obtained are shown in Table 1.

In terms of the experimental results, the precision and recall indicators under several scenarios do not show any serious deviation, and the values of the indicators except the training time are above 90%, and the classification results of the model are credible.

Further analysis of the experimental results shows that the feature-based recognition scheme in offline mode can achieve higher recognition accuracy and can flexibly adjust the combination of features according to the actual needs; for online action recognition, the convolutional neural network algorithm can show robustness to data displacement, in fact, the expansion of the data set of the translation instead of improving the recognition performance of the network, and does not need to significantly increase the training time. , so the deep learning based scheme can better work with the simple sliding window sampling method to achieve action recognition. Meanwhile, the gray-scale map of the confusion matrix is obtained as shown in Fig. 3, and Figs. (a) and (b) are the gray-scale maps of the confusion matrix for event window + feature recognition and sliding window + deep network, respectively.

Observing the gray-scale diagram of the confusion matrix, it can be found that it is relatively easy to misjudge the two types of frisbee actions, 9-forehand punt and 10-backhand punt, under both recognition schemes. From a practical point of view, this is because the two types of frisbee movements are relatively close to each other, and the trajectory of the frisbee is a fluttering motion, the difference only lies in whether the athlete's motion is forehand or backhand.

Table 1: Performance indicator record

Scheme	Acc/%	Training time(min)	P/%	R/%	F1/%
Event window + feature recognition	98.05	12.14	97.90	97.33	97.59
Sliding window + feature recognition	93.55	91.38	93.26	93.19	93.19
Event window + depth network	95.28	8.76	95.24	95.03	95.14
Sliding window + depth network	96.86	10.54	96.27	96.09	96.18

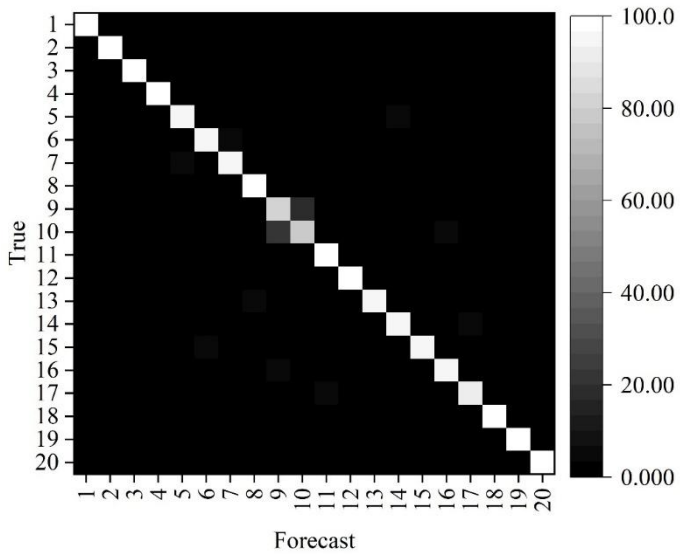

(a)The confusion matrix of the event window + feature recognition

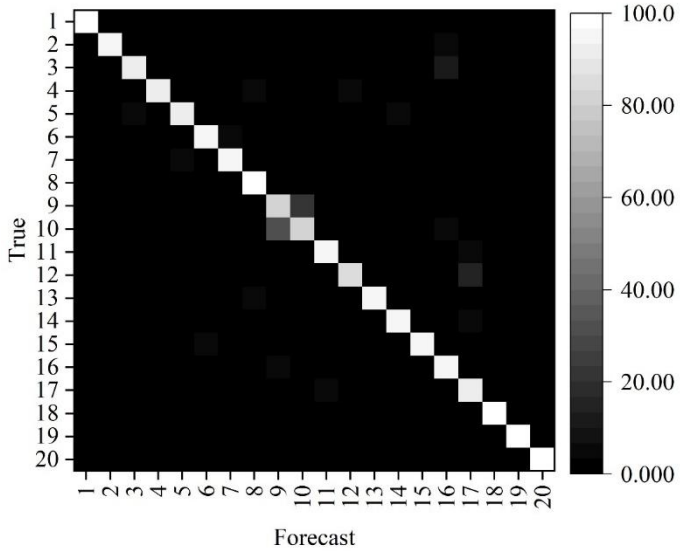

(b)Sliding window + depth network confusion matrix grayscale

Figure 3: The gray image of the confusion matrix

3.3 Action evaluation based on DTW algorithm

3.3.1 Dynamic time regularization algorithm

Dynamic Time Warping (DTW) algorithm is an algorithm to compute the optimal match between two sequences, which is often used for similarity metrics, and its main applications are in the fields of speech recognition and biometrics. In this paper, this algorithm is used to assess the similarity between two action sequences since their dimensions may be different.

Assuming that there are two time series curves B and D, applying the idea of time series to action sequences, the curves B and D are expressed as equations (14) and (15).

$$B = \left(B_1, B_2, \ldots, B_i, \ldots, B_m \right) \tag{14}$$

$$D = \left(D_1, D_2, \ldots, D_j, \ldots, D_n \right) \tag{15}$$

B represents the test sequence, D represents the standard sequence, m, n denote the number of frames of the two action sequences, B_i represents the feature vector of the i th frame, and D_j represents the feature vector of the j th frame, respectively. If and are equal, the cumulative distance is calculated directly for the two action sequences. When m and n are unequal, the DTW algorithm is used to align the two action sequences, which is done by constructing the two sequences into a matrix of $m \times n$, and the element (i, j) in the matrix denotes the distance between the corresponding points of the two action sequences and the distance between the two points of the action sequences, $d\left(B_j, D_j \right)$, which can be used according to the actual situation. , this distance can be measured in different ways according to the actual situation, here the Euclidean distance is used, as shown in equation (16).

$$d\left(B_j, D_j \right) = \sqrt{\sum_{w=1}^{N} \left(B_{iw} - D_{jw} \right)^2} \, 1 \le w \le N \tag{16}$$

The core idea of the DTW algorithm is to find the best matching path between two time series by comparing the distance between each point in the two time series, which is defined as a regularized path, denoted by W, which is the best path from point $(1,1)$ to point (m, n).

W is a continuous set of matrix elements defining the mapping between B and D. The k th element of W is defined as $w_k = (i, j)_k$, so that W can be represented by equation (17).

$$W = \left\{ w_1, w_2, \ldots, w_k, \ldots, w_k \right\} \max(m, n) \le k \le m + n - 1 \tag{17}$$

Dynamic regularization paths need to satisfy three conditions:

(1) Boundary condition: specify that the starting point of the regularization path is $W_1 = (1,1)$ and the ending point is $W_k = (m, n)$.

(2) Continuity condition: if $W_{k-1} = (a, b)$, then $W_k = \left(a', b' \right)$, which needs to satisfy $\left(a' - a \right) \le 1$ and $\left(b' - b \right) \le 1$, restricting the two points to have no empty neighbors.

(3) Monotonicity condition: if $W_{k-1} = (a, b)$, then $W_k = \left(a', b' \right)$, which needs to satisfy $\left(a' - a \right) \ge 0$ and $\left(b' - b \right) \ge 0$, restricting the points above the regularization path to proceed monotonically over time.

After the above three conditions are satisfied, there are 3 directions left for each regularization path, and if the path passes through the regularization point (i, j), the next passing point can only be one of $(i+1, j), (i, j+1), (i+1, j+1)$.

In order to obtain the optimal regularized path, the cumulative distance $A(i, j)$ is defined to be the sum of the distances between $d\left(B_j, D_j \right)$ and the nearest element that can reach this point as shown in equation (18).

$$A(i, j) = d\left(B_i, D_j \right) + \min\{ A(i-1, j-1), A(i, j-1), A(i-1, j) \} \tag{18}$$

The optimal path is the one that minimizes the cumulative distance along the path; the smaller the cumulative distance, the greater the similarity of the two action sequences.

3.3.2 Conversion of skeletal coordinates to joint angles

In order to evaluate the Frisbee sports movement, the skeletal coordinates are converted into the form of joint angles, in order to reduce the amount of calculation while providing a better representation of the movement, this paper selects the joint angles of eight joint points, the joint points are the left shoulder, the left elbow, the right shoulder, the right elbow, the left knee, the left crotch, the right knee, the right crotch, in which the angle of the joints at the left knee is represented by the left crotch, the left knee, the left ankle, and the name of the angle is recorded as θ_{lk}, and so on, the angle names of the left shoulder, left elbow, right shoulder, right elbow, left hip, right knee, and right hip are denoted by $\theta_{ls},\theta_{le},\theta_{rs},\theta_{re},\theta_{lc},\theta_{rk},\theta_{rc}$ denote the left knee angle, for example, the calculation of this angle requires the coordinate data of the left crotch, left knee, and left ankle, with $LC\left(LC_x,LC_y\right)$ denoting the left crotch coordinates, with $LK\left(LK_x,LK_y\right)$ denoting the left knee coordinates, with $LA\left(LA_x,LA_y\right)$ to denote the left ankle coordinates, and by $\mathbf{LC\_LK}\left(\mathbf{LC_x}-\mathbf{LK_x},\mathbf{LC_y}-\mathbf{LK_y}\right)$ and $\mathbf{LK\_LA}\left(\mathbf{LK_x}-\mathbf{LA_x},\mathbf{LK_y}-\mathbf{LA_y}\right)$ denotes the direction vector of the joints, and the angle is solved using the cosine theorem as shown in equation (19).

$$\theta_{lk}=\arccos\left(\frac{\mathbf{LC\_LK}\times\mathbf{LK\_LA}}{\left|\mathbf{LC\_LK}\right|\left|\mathbf{LK\_LA}\right|}\right)0°\le\theta_{lk}\le180° \tag{19}$$

Define a feature vector c_i to represent the 8 joint angle features in a certain image frame as shown in equation (20).

$$c_i=\left[\theta_{ls},\theta_{le},\theta_{rs},\theta_{re},\theta_{lk},\theta_{lc},\theta_{rk},\theta_{rc}\right] \tag{20}$$

An action sequence has multiple frames of images, defining K as the set of joint angle features of all frames, as shown in equation (21).

$$K=\left[c_1,c_2,c_3,\ldots,c_n\right] \tag{21}$$

In Eq. (21), n is the total number of image frames contained in the action sequence.

3.3.3 Dynamic time-regularized action-based evaluation analysis

In this paper, the DTW algorithm introduced above was used to calculate the DTW distance between the test action sequences and the standard action sequences as a similarity evaluation parameter, and eight joint angle features were chosen for the feature parameters to reduce the computational effort, which were right shoulder, right elbow, left intermediate, left elbow, right hip, right knee, left hip and left knee. The first of the eight movements in the dataset was chosen as the evaluation object, 40 samples were selected as the test action sequence, and the video data of the frisbee movements of the students majoring in physical education were used as the standard action sequence template. In this paper, the joint angle distance distribution is observed by multiple operations, and Figure 4 shows the DTW distance distribution of the left elbow and

the left knee, from which it can be seen that most of the DTW distances of the left elbow angle are distributed between 700 degrees and 1200 degrees, and a few are distributed between 1200 degrees and 1500 degrees; most of the DTW distances of the left knee angle are distributed between 300 degrees and 700 degrees, and a few are distributed between 700 degrees and 1300 degrees.

Figure 5 shows the distribution of DTW distances for the left shoulder and left hip, from which it can be seen that most of the DTW distances for the left shoulder angle are distributed between 400 degrees and 900 degrees, and a few are distributed between 900 degrees and 1,100 degrees; most of the DTW distances for the left hip angle are distributed between 200 degrees and 400 degrees, and a few are distributed between 400 degrees and 600 degrees, and the values that are outside these intervals are discarded.

The distribution of DTW distances for right shoulder and right hip, right elbow and right knee are shown in Figures 6 and 7, respectively. From the DTW distances in the figures, it can be seen that the distribution of the distances of the four joint points of the upper limbs is relatively sparse, and the distribution of the distances of the four joint points of the lower limbs is relatively dense, which indicates that the amplitude of the movements of the upper limbs is larger.

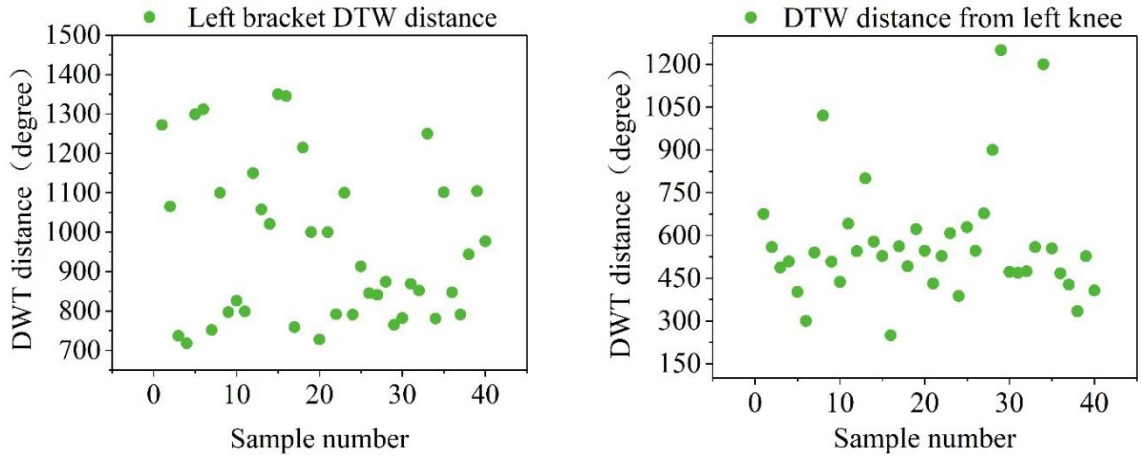

(a)Left bracket DTW distance distribution (b)The left knee DTW distance distribution

Figure 4: Left elbow and left knee DTW distance distribution

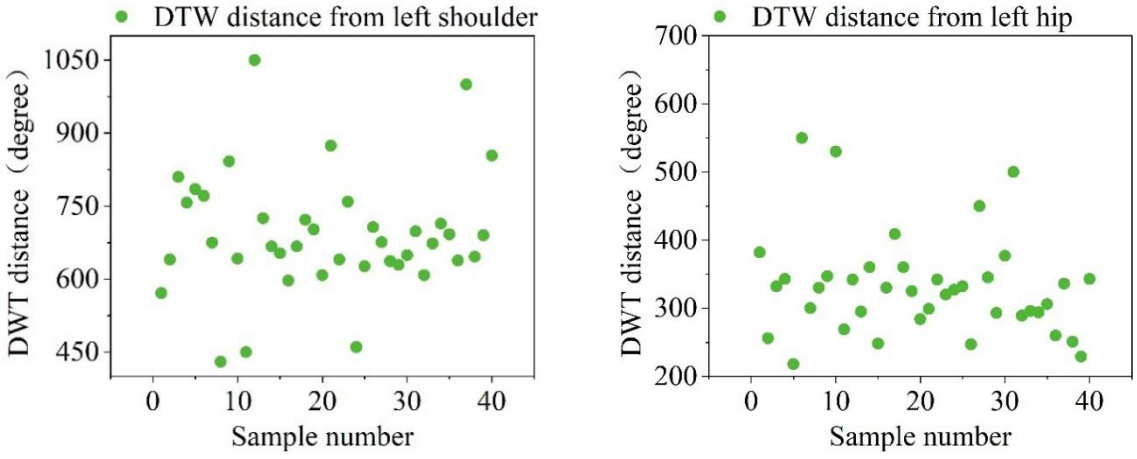

(a)Left shoulder DTW distance distribution (b)Left hip DTW distance distribution

Figure 5: Left shoulder and Left hip DTW distance distribution

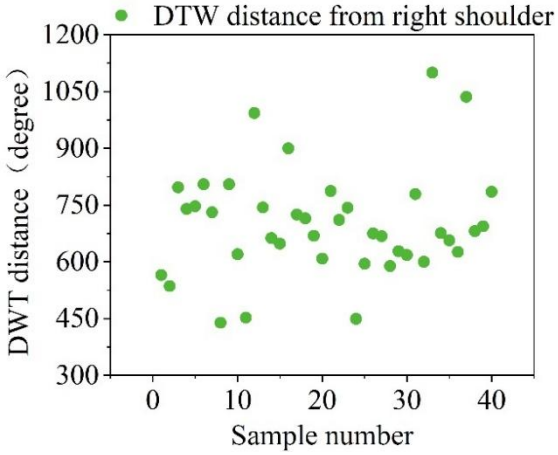

(a)Right shoulder DTW distance distribution

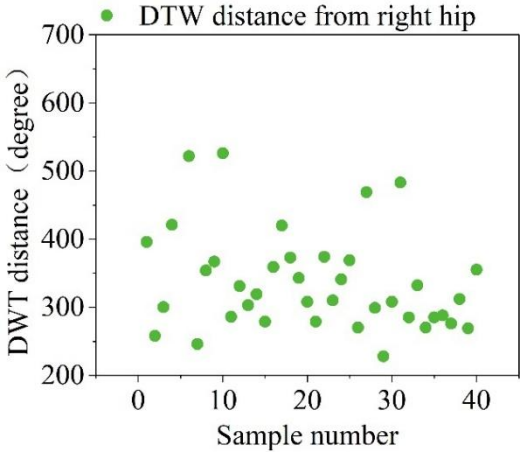

(b)Right hip DTW distance distribution

Figure 6: Right shoulder and right hip DTW distance distribution

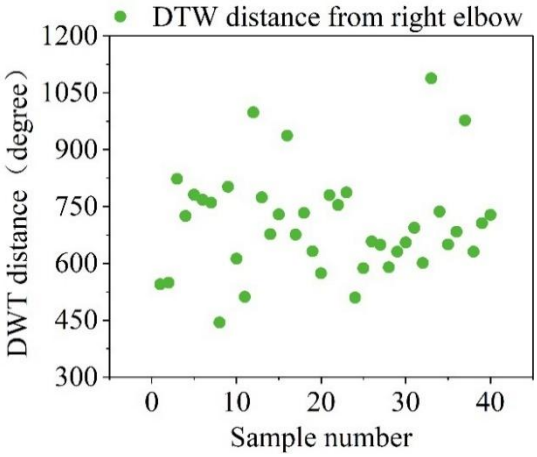

(a)Right elbow DTW distance distribution

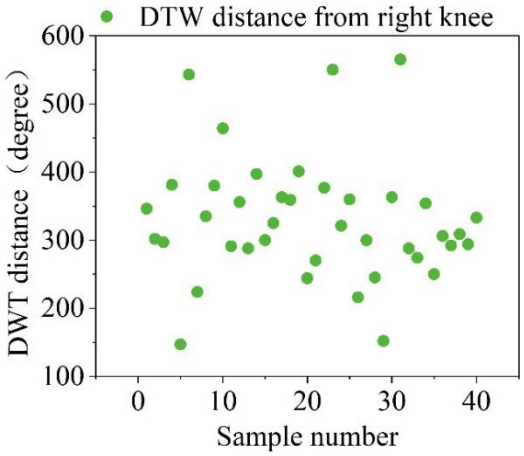

(b)Right knee DTW distance distribution

Figure 7: Right elbow and right knee DTW distance distribution

Based on the above experimental analysis, the evaluation method is constructed for the action as sealed, with the following formula:

$$s_a = s_c - (d_1 - d_2) \times f_c \tag{22}$$

where s_a denotes the score of an angular feature and s_c denotes the score of the angular assignment. d_1 denotes the DTW distance value, and d_2 denotes the minimum value within the valid interval of the DTW distance. f_c is the loss parameter, and the size of its value is related to the magnitude of the movement change, with a small loss parameter for joints with large magnitude and a large loss parameter for joints with small magnitude. The final total score is the sum of 8 joint angle scores, i.e.:

$$S = \sum_{a=1}^{8} s_a \tag{23}$$

Each joint angle has DTW distance distribution interval, after many experiments to get the base value of DTW distance for different joint angles and the loss parameters of joint points,

and finally brought into the formula to get the score of action evaluation, the results of action evaluation are shown in Table 2, which gives the evaluation results of one of the frisbee action samples, which gives the corresponding DTW distance values of eight joints and the evaluation scores and professional scoring results of this paper, respectively. Scoring results, the total score of the joints is 100 points, the total evaluation score of this paper's method is 87.2 points, and the professional score is 87.9 points, which is 0.7 points different from the professional score.

Table 2: Action evaluation results

Joint Angle name	DTW distance	Evaluation score	Professional rating
Right shoulder	987	10.4	10.3
Left shoulder	1019	10.8	10.4
Right elbow	1166	11.6	12.1
Left elbow	1380	10.7	11.1
Right hip	446	11.5	11.8
Left hip	486	11.3	10.8
Right knee	585	11.1	11.2
Left knee	781	9.8	10.2

4 Implementation of AI Assistant Teaching System for Frisbee Physical Education Classes in Private Colleges and Universities

4.1 Experimental design

4.1.1 Selection and production of experimental equipment

According to the experimental requirements, we chose the corresponding automatic Frisbee transmitter, inertial motion capture system, and optical motion capture system, and treated the reflectivity of the Frisbee. The weight of the Frisbee after covering the reflective material is on the high side compared with the ordinary Frisbee, and the corresponding other indexes, such as elasticity and inertia, will have slight changes. However, after a short period of adaptation, trainees are generally able to get used to the changes in the Frisbee.

4.1.2 Subject Recruitment Requirements and Results

The subjects' frisbee skill levels needed to have some variability in the quality of the retrieved frisbee and the standardization of the movements in order to validate the system's discriminability for different levels of subjects. After communicating with school frisbee coaches and high-level athletes, we categorized the common frisbee populations in schools by using school personnel as representatives of the target groups for the system design. In addition, the subject population should try to cover different gripping styles, different genders, and different ages in order to verify the effectiveness of the system's application in the generalized population. A total of 10 subjects were recruited according to this requirement, and four of them were selected as the analysis sample for the next data analysis.

4.1.3 Experimental Programs and Procedures

The experiment required each trainee to receive a Frisbee launch at three different levels of difficulty (slight topspin, strong topspin, and bottomspin) in order to differentiate between

trainees' level differences. Specifically for a given difficulty, the frisbee launcher was set to fire a fixed-point frisbee and sent to the trainee's forehand position to ensure that the lowest-level trainee could effectively retrieve the frisbee at the lowest difficulty. Trainees were required to return 7-10 discs to the diagonal, centerline edge, and same-side edge corners of the opposite side of the disc table, with priority given to ensuring that the returned discs would land on the table. The three target landing points are set to further differentiate the level of play between trainees. In general, it was easier to return a Frisbee to the center of the opposite table than to the edge, and easier to return a Frisbee to the diagonal than to the ipsilateral edge corner. The 7-10 frisbee launches per drop point are set to minimize the impact of trainee errors.

4.2 Analysis of the results of AI assistants in frisbee sports classes

4.2.1 Frisbee Transmitter Parameter Setting and Outgoing Frisbee Error Checking

By adjusting the two parameters of the OUKEI automatic frisbee launcher, topspin speed and bottomspin speed, it is possible to realize the realization of three preset frisbee launching difficulties: slight topspin, strong topspin and bottomspin. In more than 200 experiments, we counted the maximum and minimum variance of each characteristic corresponding to the three difficulties of Frisbee launching, and the three parameter settings and their minimum and maximum outgoing indicator variances are shown in Table 3. In the case of a fixed position of the disc transmitter, the landing point distribution of the emitted discs can comprehensively reflect the variance of the curvature, flight time and other metrics. Figure 8 shows the landing point distributions of the three difficulty disc launches received by Trainee No. 1, and the stability of the disc launches of the slight topspin and bottomspin is better than that of the strong topspin, and the minimum flight time variance of the strong topspin reaches 0.06, which is much higher than that of the slight topspin and bottomspin. It can be guessed that smaller disc launch speeds have higher stability.

Table 3: Parameter setting and minimum and maximum disk index variance

Difficulty	Upper turning parameter	Lower rotation parameter	Cu/mm	Hd/mm	Ft/ms	Ot/mm
Slight spin	5.6	2.6	0.04/0.19	6.4/30.4	0.02/5.6	0.1/27.5
Top spin	6.0	3.0	0.09/0.14	35.6/69.7	0.01/4.4	0.1/25.6
Back spin	2.7	4.1	0.07/1.61	7.7/48.2	0.06/5.2	0.1/42.2

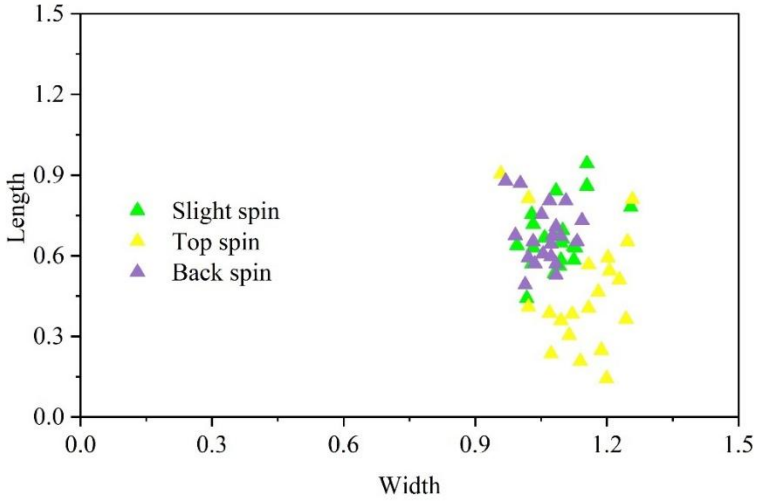

Figure 8: The different difficulty of the subject is distributed by the trainees

4.2.2 Frisbee retrieval quality analysis

The curvature Cu, the horizontal distance Hd, the flight time Ft, the offset distance Ot, and the disc acceleration Ra are not only the evaluation standard of the launching difficulty of the Frisbee, but also can be used as the reference of the Frisbee's catching level. Similarly, the smaller the value of flight time Ft, the larger the deviation Ot between the actual landing point of the disc and the expected landing point of the ideal parabola, and the larger the value of disc acceleration Ra before contacting the disc, the higher the level of disc retrieval of the trainee. The variance of the landing points of the four subjects who received the serve is shown in Table 4. In addition to the mean values of the above indicators, we also counted the success rate of the trainees' disc catching and retrieving under the three difficulties of disc launches (uptake rate, RT), and the mean values of the disc return indicators and the success rate of the four subjects' disc catching and retrieving under the slight topspin and the strong topspin and downspin launches are shown in Table 5.

Subject No. 1 scored higher in all the indicators positively related to skill level such as speed, spin and power, and was able to have a high return rate under all three serving difficulties, with a return rate of 0.70 or more under different difficulties, indicating that Subject No. 1 had the highest level among all the subjects. Similarly, it can be analyzed that subjects #3 and #4 have relatively low scores on the relevant indicators, which is consistent with the actual situation.

Table 4: Four subjects received the drop point variance

	Number1	Number2	Number3	Number4
Slight spin	1.598	3.185	0.732	4.288
Top spin	5.453	7.756	3.725	5.926
Back spin	0.977	0.965	3.795	3.294

Table 5: The index mean and the success rate of the return disk

Number	Cu/m	Hd/m	Ft/s
1	0.26/0.32/0.22	2.28/2.34/2.33	0.35/0.33/0.27
2	0.34/0.41/0.25	2.26/2.18/2.01	0.44/0.43/0.43
3	0.34/0.48/0.61	1.94/2.07/2.47	0.47/0.52/0.62
4	0.32/0.32/0.28	2.21/2.31/2.27	0.33/0.36/0.46
Number	Ot/m	Ra/m/s^2	RT
1	-0.57/-0.14/-0.23	137.0/56.7/197.0	0.76/0.78/0.71
2	0.54/-0.53/-0.74	36.8/65.8/51.7	0.81/0.52/0.56
3	-0.31/-0.23/-0.14	14.1/17.2/15.5	0.47/0.31/0.22
4	-0.23/-0.37/-0.78	82.1/73.2/48.3	0.34/0.25/0.32

To further explore the extent to which the curvature Cu, horizontal distance Hd, flight time Ft, offset distance Ot, and frisbee slap acceleration Ra of frisbee retrieval varied across frisbee retrieval outcomes, we divided all experimental rounds according to frisbee launching difficulty, with each set of frisbee launching difficulty containing data on frisbee retrieval metrics from four subjects. The scikit-learn toolkit in Python was used to do normalization and principal component analysis (PCA) on the disc catching retrieval metrics in each group of frisbee launching difficulty, and the coefficient relationships between each principal component factor and the five metrics are shown in Table 6.

The coefficient relationships between the principal components and the indicators in the slight topspin hair disc are shown in Table 7. In the slight topspin serve, the first component values differ significantly in different hitting rounds, and the main indicators constituting the

first group of principal components are curvature Cu, flight time Ft and disc acceleration Ra, with correlation coefficients of -0.533, -0.623 and 0.542, respectively.Note: The principal component values corresponding to the three types of difficulty serves are not the same, and they are listed as one line for the sake of convenience of writing here.

Table 6: Main component analysis results

	Slight spin			Top spin			Back spin		
	Var	Var ratio/%	Singular value	Var	Var ratio/%	Singular value	Var	Var ratio/%	Singular value
PC1	2.105	0.413	10.658	2.484	0.486	9.986	2.495	0.487	10.094
PC2	1.335	0.262	8.486	1.335	0.261	7.313	1.709	0.333	8.362
PC3	1.287	0.252	8.332	0.743	0.145	4.556	0.55	0.107	4.775
PC4	0.232	0.045	3.568	0.522	0.102	3.567	0.292	0.057	3.488
PC5	0.14	0.027	2.684	0.027	0.005	1.091	0.08	0.016	1.783

Table 7: The relationship between the main component and the index

	Cu	Hd	Ft	Ot	Ra
PC1	-0.533	0.024	-0.623	0.201	0.542
PC2	-0.130	0.370	0.266	-0.760	0.441
PC3	-0.501	-0.777	0.180	-0.313	-0.132
PC4	0.494	-0.455	0.216	0.174	0.683
PC5	-0.458	0.225	0.676	0.508	0.135

4.2.3 Assessment of movement standards

The trainee's body movements are temporally correlated with the disc-striking round, i.e., the assessment of movement standardization refers to the assessment of movements corresponding to a particular disc-striking round. This property is specified in Figure 9, which shows the moment point of the trajectory of the frisbee under the same round time slot with the right arm extension of Trainee #1. The absolute value of the extension angle increases, reflecting the forward swing of the trainee's arm, and the maximum moment of the extension angle corresponds to the moment of the disc strike, when the extension angle is 31.8, which is consistent with the actual situation and proves that the system and algorithm designed in the paper are effective. It lays a good foundation for more comprehensive and accurate sports evaluation and sports feedback of Frisbee sports class in private colleges and universities afterwards.

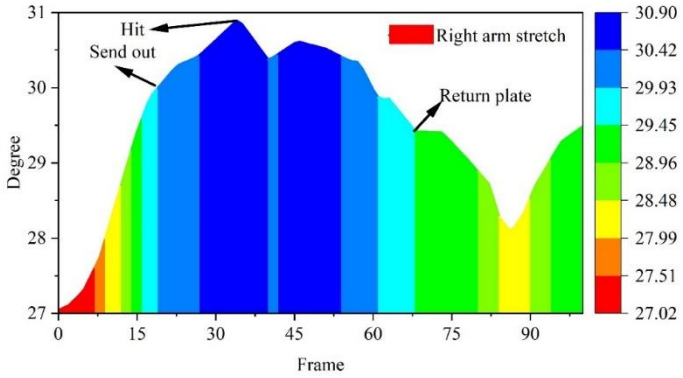

Figure 9: The trainee's right arm stretches

5 Conclusion

In order to meet the precise training needs of the AI teaching assistant system for frisbee sports classes in private colleges and universities, this study designs and validates a set of AI teaching assistant system integrating the functions of sensing, recognizing, evaluating and feedback based on the human body's key point data.

The system realizes the accurate recognition and evaluation of students' movements in the frisbee sports class of private colleges and universities, and the accuracy, precision and recall indexes of the frisbee sports movement recognition algorithm based on the spatio-temporal graph convolutional network algorithm reach more than 90%, and the total evaluation score based on the dynamic temporal regularization algorithm is 87.2, which is only 0.7 points different from that of the professionals, which verifies that this paper's movement recognition algorithm has an excellent recognition performance and the fairness of the action evaluation algorithm.

Through physiological information detection and sports equipment data detection, the AI teaching assistant system for Frisbee physical education classes in private universities can accurately reflect the differences in the level of disc skills and stability of the trained students under different disc difficulty levels of slight topspin, strong topspin, and bottomspin. In addition, the system also successfully captured the correspondence between the maximum moment of the right arm extension angle of trainee No. 1 and the moment of hitting the disc, and the extension angle at the moment of hitting the disc was the largest, with a value of 31.8, which is in line with the actual situation, which shows that the system in this paper can accurately capture the training situation of the students and give timely feedback to the physical education teachers, which reduces the workload of the teachers while providing the method of personalized training and management for the students. The system can be used to reduce teachers' workload while providing a method for personalized training and management of students.

Funding

This research was supported by the Education and Teaching Reform Research Project of Shaanxi Fashion Engineering University (project No. 2025JG0015).

About the Author

Ziyang Guo was born in Xianyang, Shaanxi, in 1996. He obtained a master's degree from Guangxi Normal University in China. He is currently working in Sports Department of Shaanxi Fashion Engineering University. He main research direction is Sports training.

Xiao Wang was born in Jingmen, Hubei, in 1993. She obtained a master's degree from Guangxi Normal University in China. She is currently working in Sports Department of Shaanxi Fashion Engineering University. Her main research directions is Higher Education.

Aoxuan Xu was born in Zibo, Shandong, in 1991. He obtained a master's degree from Guangxi Normal University in China. He is currently working in School of General Education of Guangxi Vocational University of Agriculture. His main research directions is Ethnic traditional sports science.

References

[1] Lye, C. M., & Kawabata, M. (2021). Perception of boredom in physical education lessons: What factors are associated with students' boredom experiences?. Journal of Teaching in Physical Education, 41(4), 710-719.

[2] Amoroso, J. P., Coakley, J., Rebelo-Gonçalves, R., Antunes, R., Valente-dos-Santos, J., & Furtado, G. E. (2021). Teamwork, spirit of the game and communication: a review of implications from sociological constructs for research and practice in ultimate frisbee games. Social Sciences, 10(8), 300.

[3] Xie, T., & Ma, S. (2024). Flying high and breaking stigma: a social identity perspective on Chinese frisbee participants. Leisure Studies, 1-16.

[4] Xu, H. (2025). An Empirical Study on the Impact of Ultimate Frisbee on College Students' Mental Health: Taking University Physical Education Classes as the Context. GBP Proceedings Series, 6, 19-27.

[5] Xia, Q., Han, J., Song, L., Li, H., You, K., & Cheng, L. (2025, May). Design and Implementation of an Intelligent Assisted Learning System. In 7th International Conference on Education, Network and Information Technology (p. 341). Springer Nature.

[6] Wang, S., Xu, Y., Li, Q., & Chen, Y. (2021, February). Learning path planning algorithm based on learner behavior analysis. In Proceedings of the 2021 4th International Conference on Big Data and Education (pp. 26-33).

[7] Olędzka, M., Carace, M. B., de Oliveira Tomaz, S., Pan, B., & Jiang, P. (2024). AI as a Teaching Assistant: An Innovative Approach to Education Through Customized Model Answer Generation and Guided Practice. Studia Edukacyjne, (74), 67-79.

[8] Almusawi, H. A., Durugbo, C. M., & Bugawa, A. M. (2021). Innovation in physical education: Teachers' perspectives on readiness for wearable technology integration. Computers & Education, 167, 104185.

[9] Paiva, R., & Bittencourt, I. I. (2020, June). Helping teachers help their students: A human-ai hybrid approach. In International conference on artificial intelligence in education (pp. 448-459). Cham: Springer International Publishing.

[10] Chen, Y., Deng, H., Chen, C. H., & Chung, C. L. (2023, July). Efficient artificial intelligence-teaching assistant based on chatgpt. In 2023 International Conference on Smart Systems for applications in Electrical Sciences (ICSSES) (pp. 1-5). IEEE.

[11] Chandrakant, N. S. M. (2025). AI-powered teaching assistants: Enhancing educator efficiency with NLP-based automated feedback systems. International Journal of Science and Research Archive, 14(3), 009-018.

[12] Zhang, X., Geng, J., Chen, Y., Hu, S., & Huang, T. (2023, March). I-assistant: an intelligent teaching assistant system for classroom teaching. In 2023 IEEE 12th International Conference on Educational and Information Technology (ICEIT) (pp. 1-5). IEEE.

[13] Yang, Y., Zhang, H., & Jiang, Y. (2025). An Intelligent Teaching Assistant System for Enhanced Online Engineering Education: A Dual‐Teacher Model. Computer Applications in Engineering Education, 33(6), e70098.

[14] ZhaoriGetu, H., & Li, C. (2024). Innovation in physical education teaching based on biomechanics feedback: Design and evaluation of personalized training programs. Molecular & Cellular Biomechanics, 21(2).

[15] Gao, Y. (2025). The role of artificial intelligence in enhancing sports education and public health in higher education: innovations in teaching models, evaluation systems, and personalized training. Frontiers in Public Health, 13, 1554911.

[16] Huang, Q., & Li, L. (2024). Using Deep Learning Algorithms to Generate Personalized Training Plans for Taekwondo Competitions of Physical Education Majors. World Scientific Research Journal, 10(7), 65-74.

[17] Liu, D., Sun, X., & Zhang, A. (2024). A031: Design and Practice of AI-Powered Precision Teaching Model for Public Physical Education Courses in Universities. International Journal of Physical Activity and Health, 3(3), 31.

[18] Xie, M. (2021). Design of a physical education training system based on an intelligent vision. Computer Applications in Engineering Education, 29(3), 590-602.

[19] Yeo, Z., & Chew, S. K. (2024, December). UltiVision: A Deep Learning Computer Vision Approach for Error Detection in Ultimate Frisbee Forehand Throws. In 2024 6th International Conference on Control and Robotics (ICCR) (pp. 361-365). IEEE.